Cell Reports

Article

TNFR2$^+$ regulatory T cells protect against bacteremic pneumococcal pneumonia by suppressing IL-17A-producing γδ T cells in the lung

Graphical abstract

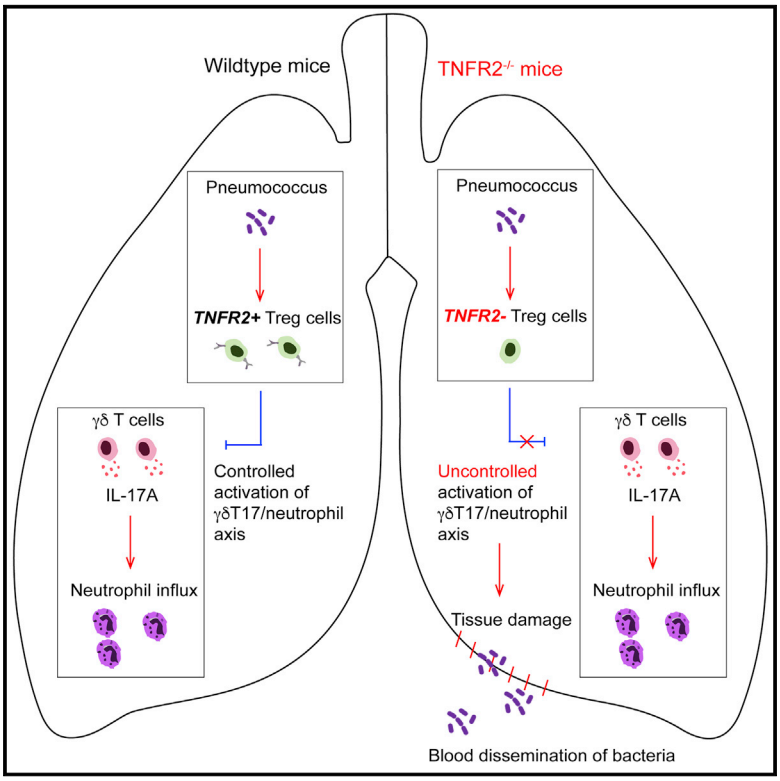

Highlights

- Pneumococcus activates lung Treg cells with upregulated TNFR2
- TNFR2$^+$ Treg cells are associated with resistance to pneumococcal infection
- TNFR2$^+$ Treg cells specifically suppress pulmonary IL-17A-producing γδ T cells
- Dysregulated γδT17 response correlates with excessive neutrophil influx to the lung

Authors

Rong Xu, Laura C. Jacques, Shadia Khandaker, ..., Neil French, Daniel R. Neill, Aras Kadioglu

Correspondence

a.kadioglu@liverpool.ac.uk

In brief

Xu et al. show that pulmonary Treg cells are activated by pneumococci via TNFR2, and lack of Treg cells or TNFR2 promotes bacterial dissemination from lungs to blood. TNFR2$^+$ Treg cells confer resistance to pneumococcal infection by controlling pulmonary γδT17 cell responses and neutrophil recruitment.

Xu et al., 2023, Cell Reports *42*, 112054
February 28, 2023
https://doi.org/10.1016/j.celrep.2023.112054

CellPress

Cell Reports

CellPress
OPEN ACCESS

Article

TNFR2$^+$ regulatory T cells protect against bacteremic pneumococcal pneumonia by suppressing IL-17A-producing γδ T cells in the lung

Rong Xu,[1] Laura C. Jacques,[1] Shadia Khandaker,[1] Daan Beentjes,[1] Miguel Leon-Rios,[1] Xiaoqing Wei,[2] Neil French,[1] Daniel R. Neill,[1] and Aras Kadioglu[1,3,*]

[1]Department of Clinical Infection, Microbiology and Immunology, University of Liverpool, Liverpool L69 7BE, UK

[2]Institute of Tissue Engineering and Repair, School of Dentistry, College of Biomedical and Life Sciences, Cardiff University, Cardiff CF14 4XY, UK

[3]Lead contact

*Correspondence: a.kadioglu@liverpool.ac.uk

https://doi.org/10.1016/j.celrep.2023.112054

SUMMARY

Streptococcus pneumoniae is a pathogen of global morbidity and mortality. Pneumococcal pneumonia can lead to systemic infections associated with high rates of mortality. We find that, upon pneumococcal infection, pulmonary Treg cells are activated and have upregulated TNFR2 expression. TNFR2-deficient mice have compromised Treg cell responses and highly activated IL-17A-producing γδ T cell (γδT17) responses, resulting in significantly enhanced neutrophil infiltration, tissue damage, and rapid development of bacteremia, mirroring responses in Treg cell-depleted mice. Deletion of total Treg cells predominantly activate IFNγ-T cell responses, whereas adoptive transfer of TNFR2$^+$ Treg cells specifically suppress the γδT17 response, suggesting a targeted control of γδT17 activation by TNFR2$^+$ Treg cells. Blocking IL-17A at early stage of infection significantly reduces bacterial blood dissemination and improves survival in TNFR2-deficient mice. Our results demonstrate that TNFR2 is critical for Treg cell-mediated regulation of pulmonary γδT17-neutrophil axis, with impaired TNFR2$^+$ Treg cell responses increasing susceptibility to disease.

INTRODUCTION

Bacterial infection is commonly accompanied by an activated pro-inflammatory response at the site of infection that helps to clear the invading pathogen, but can also hasten the breakdown of mucosal surface barriers.[1] This process can facilitate pathogen penetration of host tissue and subsequent seeding of bacteria to the bloodstream and other sterile sites, leading to invasive disease.[2,3] *Streptococcus pneumoniae* (pneumococcus) is a significant cause of morbidity and mortality worldwide, causing life-threatening diseases such as pneumonia, bacteremia, and meningitis, with an annual death burden of more than 1 million. It is the leading cause of community-acquired pneumonia, with more than 20% of the cases developing bloodstream infections.[4] As an invasive pneumococcal disease, bacteremic pneumonia is associated with a high case fatality rate ranging from 14% in young adults to 50% in the elderly, despite the broad application of antibiotic treatment and prophylactic intervention with conjugated pneumococcal vaccines.[5,6] Pneumococcal infection induces a rapid influx of neutrophils to the lung, as a broad range host defense mechanism against extracellular pathogens.[7] However, by producing a large quantity of reactive oxygen species, inflammatory cytokines, and chemokines, as well as degranulation and NETosis, those infiltrating neutrophils can also cause collateral tissue damage, leading to sepsis.[8–10] Regulation of neutrophil recruitment in the lung upon pneumococcal infection is therefore required to contain a potentially detrimental pro-inflammatory response and maintain tissue integrity when clearing the bacteria.

Pulmonary γδ T cells have an important defensive role in both bacterial and viral infection.[11,12] In response to pneumococcal infection, γδ T cells are activated and express high levels of interleukin (IL)-17A and interferon (IFN)γ, contributing to bacterial clearance through promoting neutrophil recruitment and activating macrophages.[12,13] However, activation of IL-17A-producing γδ T cells (γδT17) can also cause pathological changes through over-recruitment of neutrophils, as has been demonstrated in influenza infection, skin inflammation, and breast cancer metastasis.[14–16] It is not clear how γδT17 and neutrophil responses are regulated in pneumococcal infection. Our previous study demonstrated that Foxp3$^+$ regulatory T (Treg) cell expansion in the lung of BALB/c mice is associated with their resistance to invasive pneumococcal infection, while CBA/Ca mice, which lack an effective local Treg response following infection, rapidly develop septicemia and die,[17] suggesting that Treg cells may be a key regulator in pneumococcal infection to control the pro-inflammatory responses in the lung. This is supported by another study demonstrating that the sex hormone estradiol can promote a quicker resolution of lung inflammation and injury in mice with non-invasive pneumococcal infection through enhancing Treg cell responses.[18]

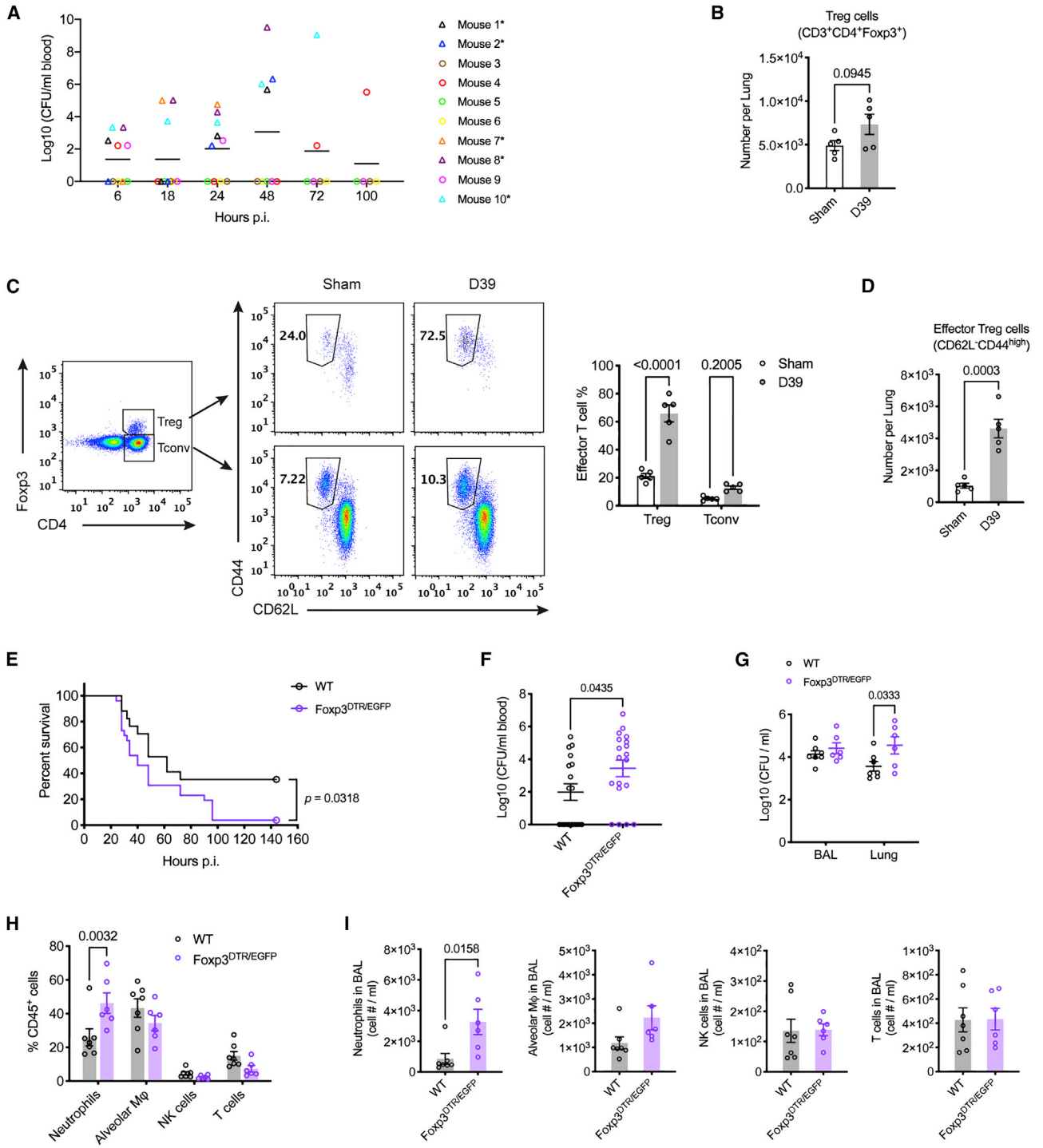

Figure 1. Treg cells are activated by pneumococcal infection and protect mice from bacteremic pneumonia

(A) Wild-type (WT) C57BL/6 mice were infected (i.n.) with D39 pneumococci and blood was collected using tail bleeding at predetermined timepoints as indicated. The blood colony-forming unit (CFU) count over time for individual mouse was plotted (individual values +mean), with each colored symbol representing one individual. Mice that were culled due to ill health are labeled with "*" next to their IDs.

(B–D) WT C57BL/6J mice were infected (i.n.) with D39 pneumococci or PBS for the sham infection group and the lungs were collected and analyzed at 18 h post infection (p.i.). (B) Number of Treg cells ($CD3^+CD4^+Foxp3^+$) in the lung of sham and D39 infected mice. (C) Representative flow cytometry plots for the frequency of effector ($CD62L^-CD44^{high}$) Treg and conventional T cells (Tconv, $CD3^+CD4^+Foxp3^-$). Data were summarized using grouped bar graph. Number of effector Treg cells is shown in (D). Data are from one (n = 5 per group) of two independent experiments.

(legend continued on next page)

Because BALB/c and CBA/Ca mice have distinct T cell profiles and differ in innate immune responses, including neutrophil recruitment, it has been challenging to interpret the cellular mechanisms mediating protection by Treg cells during pneumococcal pneumonia. In this study we uncover those mechanisms.

Tumor necrosis factor (TNF) is a potent pro-inflammatory cytokine that is upregulated in many inflammatory conditions, including pneumococcal pneumonia.[19–21] Although TNFα was initially described as an inducer of cell apoptosis and orchestrator of inflammation in response to pathogen invasion and tissue damage, it is now appreciated that it can also mediate activation of Treg cells through TNF receptor 2 (TNFR2).[22,23] Unlike the ubiquitous expression of TNFR1 across most cell types, TNFR2 is expressed in a restricted manner, predominantly on Treg cells.[24] In a mouse colitis model, Treg cells in the lamina propria require TNFR2 to maintain Foxp3 expression and a suppressive phenotype, indicating an essential role of TNFR2 in stabilizing Treg cells in an inflammatory mucosal environment.[25] Although accumulating evidence indicates an indispensable protective role of TNFR2$^+$ Treg cells in autoimmune inflammatory settings,[25–27] the influence of this receptor on the development of responses to invasive pathogens is unknown.

In the years since anti-TNFα therapy was approved for clinical treatment of rheumatoid arthritis, an interesting observation has been the higher incidence of pneumococcal infection reported among those patients receiving anti-TNF drugs, with some developing bacteremic pneumococcal pneumonia,[19,28–31] suggesting that TNFα signaling promotes resistance to invasive pneumococcal infection. This observation prompted us to investigate whether TNFα-TNFR2 signaling might be required for Treg cell activation during pneumococcal infection and to explore the role of TNFR2$^+$ Treg cells in regulating the neutrophil-dominated pro-inflammatory responses in the lung. In this study, we uncover a crucial function of TNFR2$^+$ Treg cells in controlling γδT17 cell-mediated neutrophil influx in pneumococcus-infected lungs and thereby preventing the development of lethal sepsis.

RESULTS

Treg cells are activated by pneumococcal infection and protect mice from bacteremic pneumonia

A rapid recruitment and activation of Foxp3$^+$ Treg cells in the lung after pneumococcal infection has been associated with resolution of inflammation and local containment of infection.[17,18] Following intranasal (i.n.) infection with the invasive serotype 2 pneumococcal strain D39, over 50% of C57BL/6 mice developed sepsis, with substantial bacterial load in the blood within 24 h post infection (p.i.) (Figure 1A). Five of the six mice that had blood dissemination of bacteria at 24 h p.i. eventually died of sepsis, suggesting that early regulation of inflammatory responses in the lung is critical to prevent the development of bacteremic pneumonia. We first sought to determine whether pneumococcal infection altered the Treg cell responses in the lung at 18 h p.i.. No significant change in total Treg cell numbers was observed in response to pneumococcal challenge (Figure 1B). We then examined the activation of Treg cells in pneumococcus-infected lungs by their expression of CD62L (L-selectin) and CD44, two adhesion molecules that have been used to differentiate naive (CD62L$^+$CD44^{low}) and activated/memory (CD62L$^-$CD44^{high}) T cells.[32] Interestingly, we found that Treg cells with an effector phenotype (CD62L$^-$CD44^{high}) were markedly increased both in number and frequency, whereas the activation of conventional CD4$^+$ T (Tconv) cells was not significantly altered (Figures 1C and 1D), suggesting a preferential activation of Treg cells following pneumococcal infection.

To investigate the role of Treg cells in the progression from contained local infection to systemic dissemination of bacteria, we used DEREG mice (Depletion of Regulatory T cells, Foxp3$^{DTR/EGFP}$), which carry a diphtheria toxin receptor (DTR)-EGFP transgene under the control of an additional Foxp3 promoter, enabling specific depletion of Treg cells by administration of diphtheria toxin (DT).[33] Foxp3$^{DTR/EGFP}$ mice and their wild-type (WT) littermates were given two doses of DT prior to infection with pneumococci. At the time of infection, over 90% of Treg cells were removed both in the lung and lymph nodes of the Foxp3$^{DTR/EGFP}$ mice, while frequency of Treg cell population in those WT control mice was not altered (Figure S1A). Following pneumococcal infection, Treg cell depletion resulted in a significantly lower survival (3.8%) in Foxp3$^{DTR/EGFP}$ mice, compared with their WT control littermates (35.3% survival) (Figure 1E). Correlating with the decreased survival, Foxp3$^{DTR/EGFP}$ mice had significantly increased dissemination of bacteria into blood at 18 h p.i. (Figure 1F). In addition, higher titers of pneumococci were harvested from the lung tissue of Treg cell-depleted Foxp3$^{DTR/EGFP}$ mice compared with WT controls, although they had a similar number of bacteria recovered from the bronchioalveolar lavage (BAL) (Figure 1G), suggesting that Treg cell depletion may not affect bacterial load in the airways but may promote tissue invasion of pneumococci.

Treg cells are potent immune regulators that suppress inflammatory responses and promote tissue repair. To investigate whether the higher incidence of fatal pneumococcal sepsis in Treg cell-depleted mice was associated with uncontrolled inflammation, we evaluated leukocyte infiltration in the lung of pneumococcus-infected Foxp3$^{DTR/EGFP}$ and WT control mice. DT administration reduced lung T cell numbers in the naive Foxp3$^{DTR/EGFP}$ mice but did not affect other leukocyte populations, including neutrophils, alveolar macrophages, and natural killer (NK) cells

(E–I) Foxp3$^{DTR/EGFP}$ mice and their WT littermates were infected (i.n.) with D39 pneumococci. (E) Survival of infected mice. Data were pooled from three independent experiments (n = 17 for WT mice; n = 26 for Foxp3$^{DTR/EGFP}$ mice). (F) Blood CFU count at 18 h post infection. Data from four independent experiments were pooled (n = 17 for WT mice; n = 19 for Foxp3$^{DTR/EGFP}$ mice). (G) CFU count in bronchioalveolar lavage (BAL) and lung homogenates. (H and I) Proportion (H) and number (I) of neutrophils (CD45$^+$CD11b$^+$Ly6G$^+$), alveolar macrophages (Mφ) (CD45$^+$CD11b$^{-/low}$SiglecF$^+$), NK cells (CD45$^+$CD3$^-$NKp46$^+$), and T cells (CD45$^+$CD11b$^-$CD3$^+$) in the BAL. Data were pooled from two independent experiments (n = 7 for WT mice; n = 6 for Foxp3$^{DTR/EGFP}$ mice). Unpaired two-tailed t test was used for statistical analysis in (B), (D), and (I). Data in (C), (G), and (H) were analyzed by ordinary two-way ANOVA with Sidak's multiple comparisons test. The survival curves (E) were compared by Log rank (Mantel-Cox) test. Mann-Whitney test was used to analyze data in (F). Data shown as mean ± SEM unless otherwise stated.

in either bronchioalveolar space or lung tissue (Figures S1B and S1C). Upon pneumococcal infection, a neutrophil-dominated leukocyte influx was detected in the lung (Figure S2). Prior depletion of Treg cells resulted in a significantly increased neutrophil infiltration to the airway following pneumococcal infection in Foxp3$^{DTR/EGFP}$ mice compared with their WT littermates, while recruitment of other leukocytes was not altered (Figures 1H and 1I). In the lung tissue, frequency of neutrophils was also higher in Treg cell-depleted mice upon infection, but their increase in number did not reach significance (Figure S3). This suggests that Treg cells may regulate the neutrophil influx partially by inhibiting neutrophil migration from lung parenchyma and/or vasculatures into bronchioalveolar space. Excessive neutrophil influx can breach the mucosal barrier, leading to bacterial dissemination.[8,9] Our results indicate an essential role of Treg cells in regulating neutrophil infiltration in pneumococcus-infected lungs and thereby preventing the development of bacteremia.

TNFR2 is essential to stabilize lung Treg cell population during pneumococcal pneumonia

Emerging evidence indicates that TNFR2^{+} Treg cells possess a more potent immunosuppressive function and provide protection against colitis and neuroinflammation.[25,26] TNFα activates Treg cells and stabilizes Foxp3 expression through TNFR2 signaling.[23,25] Upon pneumococcal infection, TNFα is quickly upregulated in the lung, and is primarily produced by macrophages.[20,21] An increased level of TNFα in the lung homogenate by 18 h post D39 infection was also detected in our study (Figure 2A). We therefore investigated whether TNFα-TNFR2 signal regulates the Treg cell responses in the lung during pneumococcal pneumonia. We first examined the expression of TNFR2 in pulmonary Tconv and Treg cells in naive mice. Cells isolated from the lung of TNFR2$^{-/-}$ mice were used as a negative control. TNFR2$^{-/-}$ mice have a targeted knockout on the tumor necrosis factor receptor superfamily, member 1b (*tnfrsf1b*) gene, which encodes TNFR2. As expected, TNFR2 was predominantly expressed by Treg cells in the lung of WT mice (Figure 2B), consistent with previous reports showing considerably higher expression of TNFR2 by Treg cells compared with Tconv in peripheral lymphoid tissues.[23] Post pneumococcal infection, TNFR2 expression on Treg cells was significantly upregulated (Figure 2C). TNFR2 expression on Treg cells was observed predominantly on the CD62^{-}CD44^{high} effector Treg subsets, and this cell type accounted for the increased expression observed following infection (Figure 2D), indicating that TNFR2 expression was associated with Treg cell activation by pneumococcus.

We then examined the lung Treg cells in TNFR2$^{-/-}$ mice exposed to pneumococcus to investigate whether loss of TNFR2 signaling affected the infection-induced Treg cell activation. Lung Treg cell frequency was lower in naive TNFR2$^{-/-}$ mice compared with WT control mice and this difference became more pronounced following infection (Figure 2E). Although the proportion of effector Treg cells (CD62^{-}CD44^{high}) was also increased post pneumococcal infection in TNFR2$^{-/-}$ mice, absolute numbers of both total and effector Treg cells in the lung were significantly lower than in WT animals (Figures 2F and 2G). Therefore, our results suggest that although TNFR2 signaling may be dispensable for Treg cell activation, it is essentially required to maintain activated pulmonary Treg cells in response to pneumococcal infection.

Deficiency in TNFR2 results in high susceptibility to pneumococcal infection

Our data show that Treg cell-mediated regulation prevents excessive neutrophil infiltration during pneumococcal infection, and that TNFR2 deficiency significantly diminishes the Treg cell population in infected lungs. We therefore hypothesized that TNFR2$^{-/-}$ mice, lacking TNFR2^{+} Treg cells, would demonstrate enhanced susceptibility to pneumococcal infection. Indeed, upon intranasal challenge with D39 pneumococci, all TNFR2$^{-/-}$ mice rapidly developed bacteremia and succumbed to infection, while 38.5% of WT mice survived (Figure 3A). This was accompanied by significantly increased bacterial load in the lung tissue and blood circulation in TNFR2$^{-/-}$ mice by 18 h p.i., mirroring their rapid progress to bacteremic pneumonia p.i. (Figures 3B and 3C). As we had previously observed in Treg cell-depleted DEREG mice, bacterial numbers in the bronchioalveolar space were comparable between WT and TNFR2$^{-/-}$ mice (Figure 3B).

Thus, upon pneumococcal infection, TNFR2-deficient mice rapidly developed invasive disease, with quick progression of bacterial dissemination from lungs to blood. To investigate whether this was associated with dysregulated neutrophil infiltration, as seen in Treg cell-depleted DEREG mice, we examined histopathology and leukocyte populations in the lungs of TNFR2$^{-/-}$ mice post intranasal inoculation of pneumococci. By 18 h, histology of pneumococcus-infected lungs showed heavy perivascular and peribronchial accumulation of leukocytes in TNFR2$^{-/-}$ mice, consisting mainly of neutrophils, indicating acute inflammation (Figure 3D). Analysis of cells recovered from the bronchioalveolar space and lung tissue confirmed that this markedly enhanced inflammation was predominantly due to increased recruitment of neutrophils into lungs of TNFR2$^{-/-}$ mice, compared with WT control mice (Figures 3E, 3F, S4A, and S4B). In addition, a small, but significant, increase in NK cell recruitment in TNFR2$^{-/-}$ mice was also detected (Figure 3F). Infected lungs from WT mice were substantially less inflamed, with minimal evidence of inflammation or leukocyte infiltration. Significantly increased neutrophil recruitment in TNFR2$^{-/-}$ mice was apparent as early as 6 h p.i., when their lung and blood bacterial loads were still comparable to the WT mice (Figures S4C–S4E).

Collectively, our data show excessive neutrophilic inflammation and rapid development of bacteremia following pneumococcal infection in TNFR2-deficient mice, which is associated with impaired pulmonary TNFR2^{+} Treg responses.

Accumulation of $\gamma\delta$T17 cells in the lungs of pneumococcus-infected TNFR2$^{-/-}$ mice

IL-17A is a pro-inflammatory cytokine that induces granulopoiesis and neutrophil migration to inflammation sites,[34] while activation of IL-17A-producing $\gamma\delta$T17 cells is associated with neutrophil recruitment in the lung.[35,36] Post infection with D39 pneumococci, upregulated mRNA expression of IL-17A was detected in T cells from infected lungs as early as 6 h p.i. and peaking at 12 h p.i. in the WT mice (Figure 4A). In accordance with increased IL-17A mRNA expression in the early response to pneumococcus, the

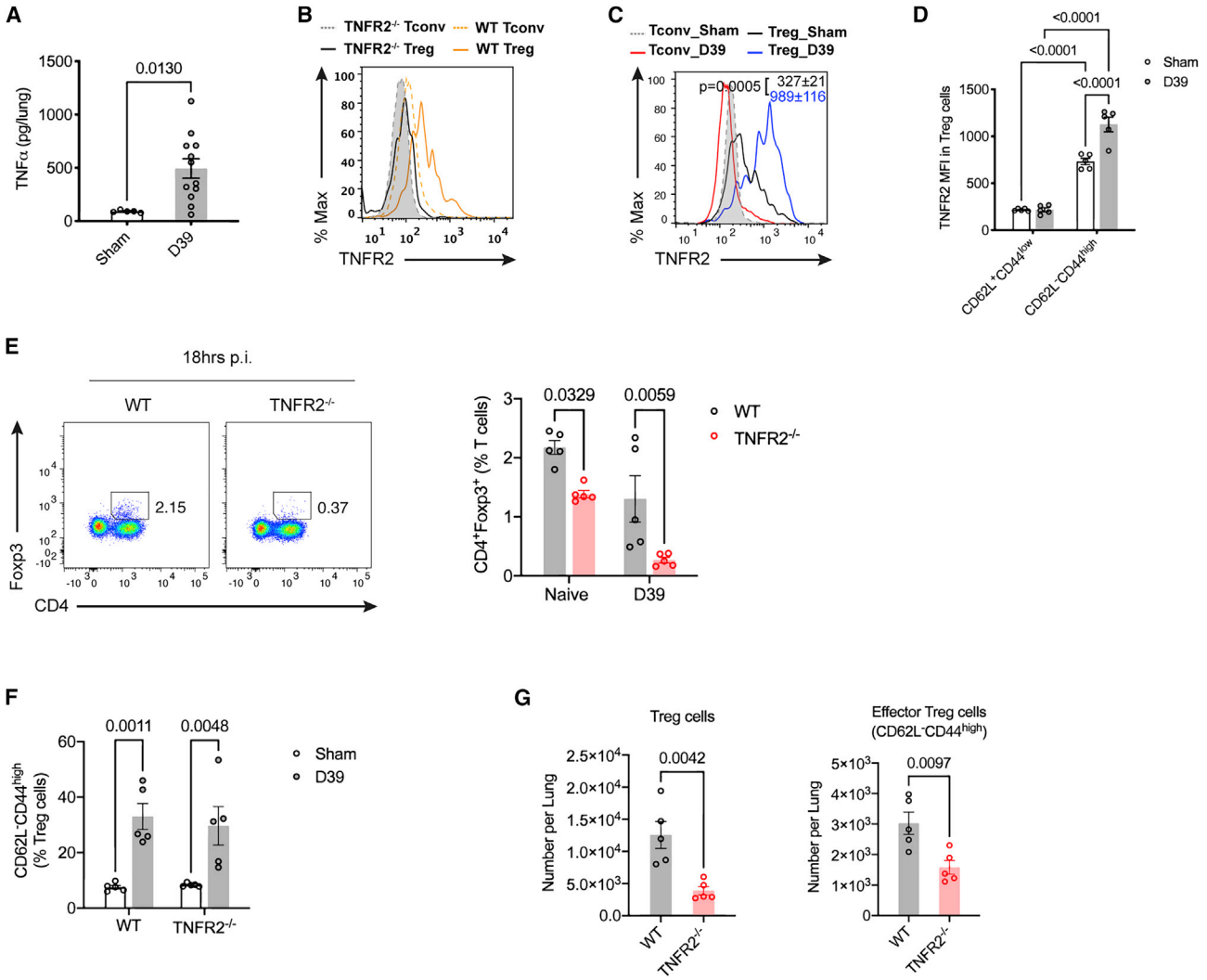

Figure 2. TNFR2 is essential to stabilize lung Treg cell population during pneumococcal pneumonia

(A) WT C57BL/6J mice were i.n. inoculated with PBS (sham infection) or D39 pneumococci. The concentration of TNFα in the lung homogenate measured at 18 h p.i. Data were pooled from two independent experiments (Sham: n = 5 mice; Infected: n = 12 mice).

(B) Flow cytometry histogram showing the expression level of TNFR2 in Tconv and Treg cells from the lung of naive mice. Tconv (dashed gray line and shadowed) and Treg (black line) cells from TNFR2$^{-/-}$ mice were used as negative staining controls for the comparison of TNFR2 expression in Tconv (dashed orange line) and Treg (orange line) cells from WT mice. Representative plot of n = 3 mice.

(C–G) Mice were infected with (i.n.) D39 pneumococcus and lung T cell activation was analyzed at 18 h p.i.

(C) Representative flow cytometry histogram to compare TNFR2 expression level in lung Tconv and Treg cells with or without D39 infection, with the median fluorescence intensity (MFI) ± SEM for Treg cells indicated on the top right corner, in WT mice.

(D) TNFR2 MFI in naive (CD62L^{+}CD44^{low}) and effector (CD62L^{-}CD44^{high}) Treg cells in the lung of D39 infected WT mice compared with sham infection, n = 5 mice per group.

(E) Representative flow cytometry plots for Treg cell frequency (gated on CD3^{+} T cells) in the lung of pneumococcal-infected mice and summarized proportion of Treg cells in WT and TNFR2$^{-/-}$ mice with or without infection.

(F) Percentage of effector Treg cells in the lung of D39 infected WT or TNFR2$^{-/-}$ mice compared with sham infected mice.

(G) Number of total and effector Treg cells in D39 infected lungs. n = 5 mice per group. Unpaired two-tailed t test was used for data analysis in (A), (C), and (G). Data were analyzed by ordinary two-way ANOVA with Sidak's multiple comparisons test in (D)–(F).

number of IL-17A^{+} T cells was also increased in the lung by 18 h p.i. (Figure 4B). In addition, IFNγ^{+} T cell activation was also detected in infected lungs (Figure 4B).

TNFR2 deficiency resulted in a significant increase in neutrophil infiltration in pneumococcus-infected lungs. We next sought to determine whether this was related to dysregulated IL-17A responses in lung T cells. In TNFR2$^{-/-}$ mice, total T cell numbers and CD4^{+} T cell numbers in pneumococcus-infected lungs were comparable to the WT control mice. However, a significant increase of γδ T cells was detected in the lung of TNFR2$^{-/-}$ mice

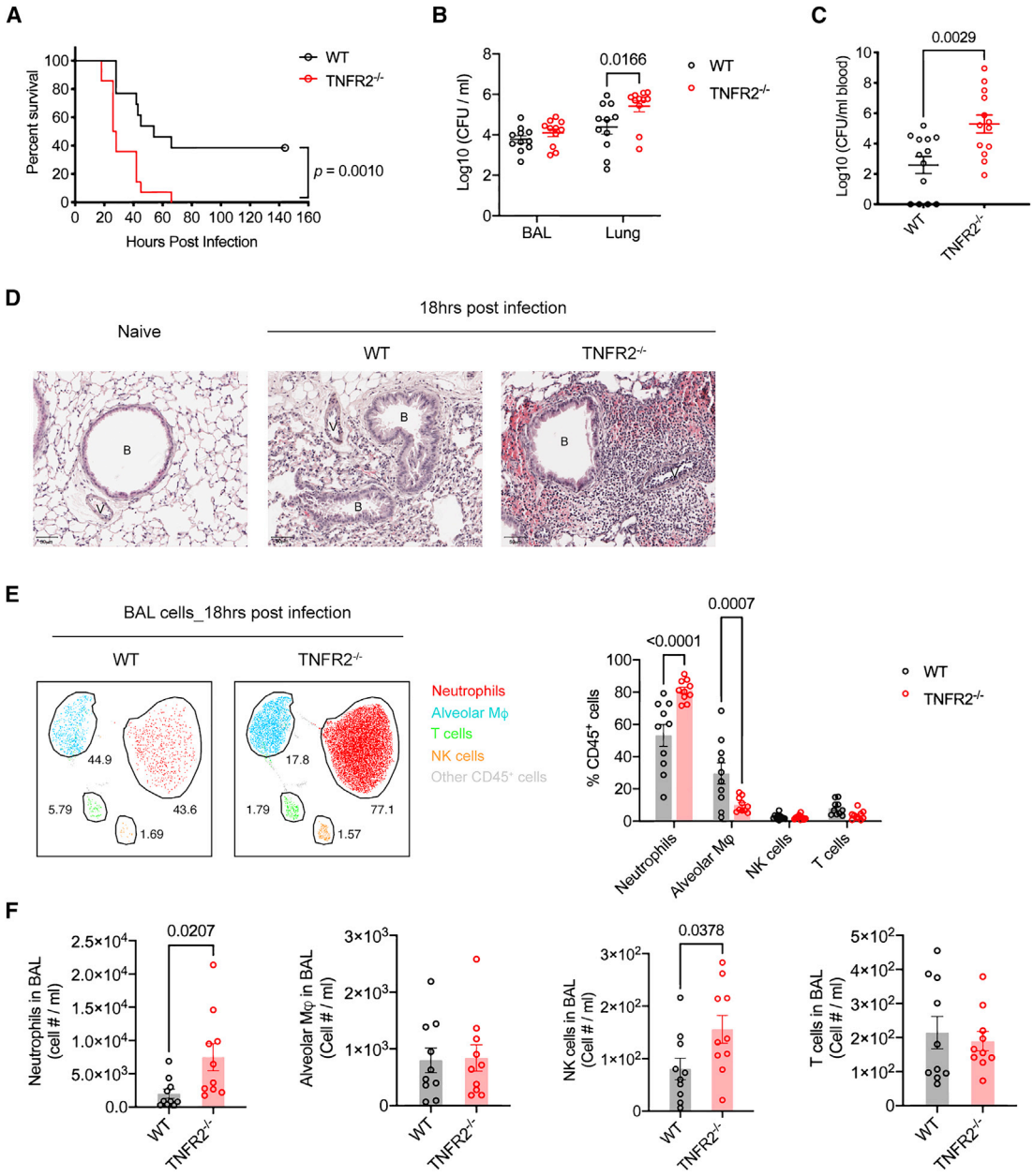

Figure 3. Deficiency in TNFR2 results in high susceptibility to pneumococcal infection

(A–F) WT and TNFR2$^{-/-}$ mice were inoculated (i.n.) with D39 pneumococci and analyzed at 18 h p.i.

(A) Survival of infected mice. Data were pooled from two independent experiments (WT mice, n = 13; TNFR2$^{-/-}$ mice, n = 14). Log rank (Mantel-Cox) test was used to compare the survival curves.

(B) Bacterial count in the BAL and lung homogenates, with data pooled from two independent experiments (n = 11 mice per group).

(C) Bacterial count in the blood. Data were pooled from two independent experiments (n = 13 mice per group).

(D) Lung histology images (hematoxylin and eosin staining) from naive (represents n = 3 WT mice) and infected (WT and TNFR2$^{-/-}$, represents n = 4 mice per group) mice. Scale bars, 50 μm. B, bronchiole; V, vasculature.

(E) Representative flow cytometry UMAP plots for the frequency of neutrophils (red), alveolar Mϕ (light blue), T cells (green), NK cells (orange), and other CD45^{+} cells (gray) in the BAL of infected mice. Data were summarized using grouped bar graph, pooled from two independent experiments (n = 10 mice per group). Number of those leukocyte populations in the BAL is shown in (F). Data in (B) and (E) were analyzed by ordinary two-way ANOVA with Sidak's multiple comparisons test. Unpaired two-tailed t test was used for the statistical analysis in (C) and (F).

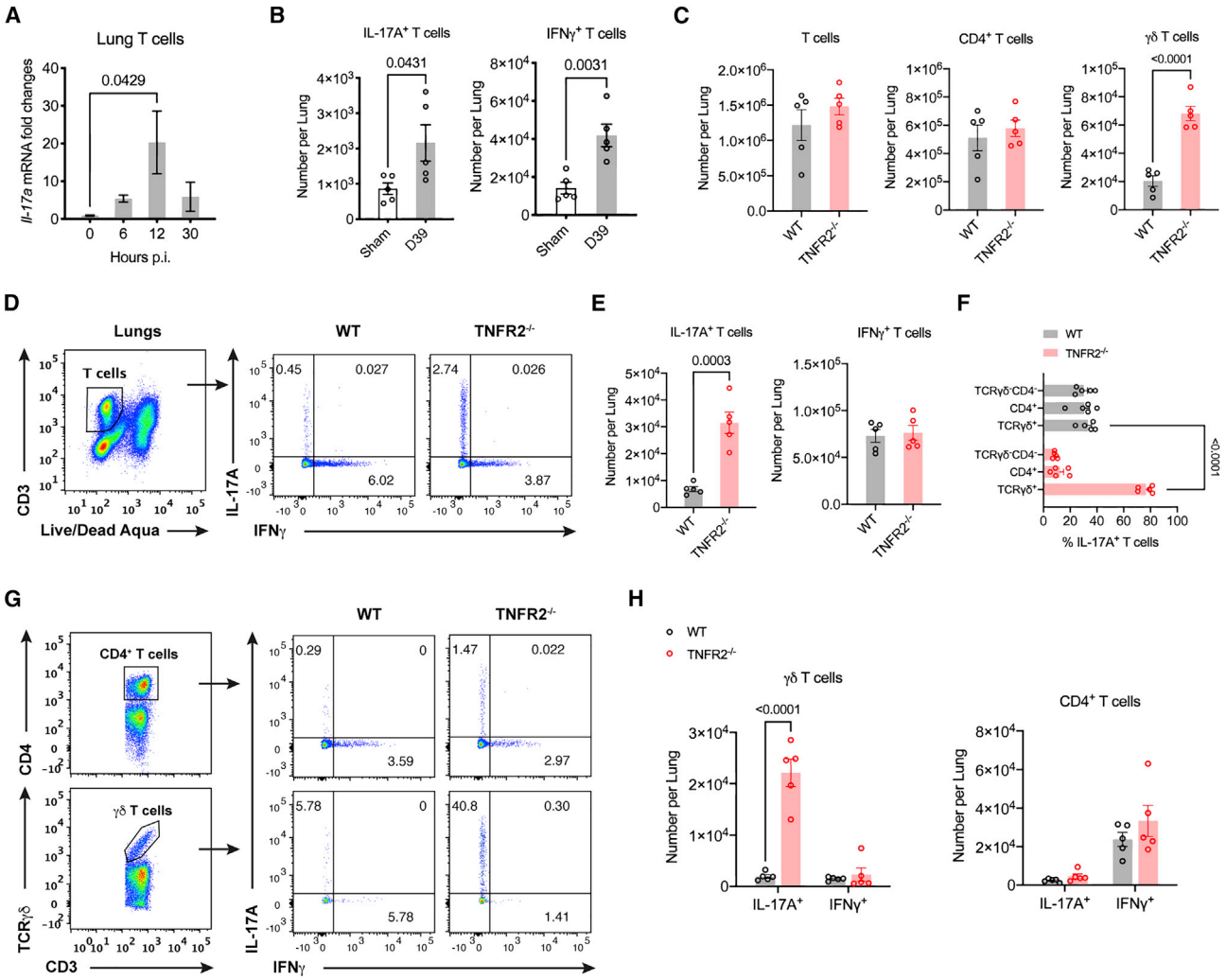

Figure 4. Accumulation of γδT17 cells in the lung of pneumococcus-infected TNFR2$^{-/-}$ mice

(A and B) WT C57BL/6J mice were infected (i.n.) with D39 pneumococci.

(A) Lung T cells were separated at 0, 6, 12, and 30 h p.i. for the measurement of *Il17a* mRNA expression. Six infected mice were culled per time point and the lung T cells from three mice were pooled for total RNA extraction. qPCR was done in duplicate. Kruskal-Wallis test (ANOVA) with Dunn's multiple comparisons test was used for the statistical analysis.

(B) Number of IL-17A$^+$ and IFNγ$^+$ T cells in the lung of sham or D39 infected mice at 18 h p.i., n = 5 mice per group.

(C–H) WT and TNFR2$^{-/-}$ mice were inoculated (i.n.) with D39 pneumococci and analyzed at 18 h p.i.

(C) Number of CD3$^+$ T cells, CD3$^+$CD4$^+$ T cells, and CD3$^+$TCRγδ$^+$ γδ T cells in the lung.

(D–F) Representative flow cytometry plots for IL-17A and IFNγ expression in live CD3$^+$ T cells (D) and number of IL-17A$^+$ and IFNγ$^+$ T cells in the lung (E), with frequency of TCRγδ$^+$, CD4$^+$, and TCRγδ$^-$CD4$^-$ cells in IL-17A$^+$ T cells shown in (F).

(G and H) Representative flow cytometry plots for IL-17A and IFNγ expression in CD3$^+$CD4$^+$ and CD3$^+$TCRγδ$^+$ T cells (G) and number of IL-17A$^+$ and IFNγ$^+$ cells in γδ and CD4$^+$ T cells respectively (H). Data represent one of two independent experiments (n = 5 mice per group). Unpaired two-tailed t test was used for the analysis of data in (B), (C), and (E). Ordinary two-way ANOVA with Sidak's multiple comparisons test was used to analyze data in (F) and (H).

(Figure 4C). Interestingly, we found that TNFR2 deficiency further promoted activation of IL-17A but not IFNγ-producing T cells in the lung during pneumococcal infection (Figures 4D and 4E). Of those T cells found to be producing IL-17A, more than 75% were γδ T cells in TNFR2$^{-/-}$ mice, compared with an average of 33.2% in WT mice (Figure 4F), suggesting unregulated activation of γδT17 cells in TNFR2-deficient mice. This was further confirmed by examining IL-17A and IFNγ expression in CD4$^+$ and γδ T cells, where a markedly increased proportion of IL-17A$^+$ cells in the γδ T cell subset and remarkably higher number of γδT17 cells in the lung of infected TNFR2$^{-/-}$ mice was observed, while the frequency of γδ T cells expressing IFNγ was reduced compared with the WT mice (Figures 4G and 4H). Lung CD4$^+$ T cells also upregulated IL-17A in the absence of TNFR2$^+$ Treg cells, but this increase was not significant (Figure 4G). Hence, these results suggest that TNFR2 signaling is

required to control γδT17 cell activation in the lung during pneumococcal infection, and this effect may be mediated through Treg cell responses.

TNFR2$^+$ Treg cells suppress γδT17 cells in pneumococcus-infected lungs

Our results obtained from TNFR2$^{-/-}$ mice suggest that γδT17 activation in pneumococcus-infected lungs might be controlled by TNFR2$^+$ Treg cells. To examine whether a general depletion of Treg cells would also lead to highly elevated γδT17 activation in pneumococcal infection, we examined T cell responses in the lung of Foxp3$^{DTR/EGFP}$ mice that were depleted of Treg cells by DT administration. Post infection, expression of both IL-17A and IFNγ were higher in lung T cells in the absence of Treg cells (Figure 5A). An increase in the proportion of IL-17A$^+$ γδ T cell cells was also detected (Figure 5B), confirming Treg cell-mediated regulation of γδT17 cells in the TNFR2-deficient mice. However, a more prominent activation of IFNγ-producing CD4$^+$ T cells (Th1) in the lung of Treg cell-depleted mice was observed upon pneumococcal infection (Figures 5C–5E). This suggests that members of the total lung Treg cell population function for the regulation of Th1 cell activation, while TNFR2$^+$ Treg cells specifically control γδT17 cells. The highly activated Th1 responses in the lung of Treg cell-depleted mice may have an influence on the activation of γδT17 cells, hence the lung γδT17 response in those mice was not augmented as significantly as was seen in the TNFR2$^{-/-}$ mice.

To confirm our hypothesis that TNFR2$^+$ Treg cells regulate the activation of γδT17 cells in the lung during pneumococcal pneumonia, TNFR2$^+$ Treg cells isolated from WT mice were intravenously (i.v.) transferred into TNFR2$^{-/-}$ mice 24 h prior to intranasal infection of pneumococcus. As expected, only IL-17A but not IFNγ-producing γδT cells were suppressed during infection, shown as reductions in both frequency and number, in the lung of mice receiving TNFR2$^+$ Treg cells (Figures 5F and 5G). The proportion of Th1 cells was also decreased, but their number in the lung was not significantly lower (Figures 5H and 5I). In addition, the adoptive transfer of TNFR2$^+$ Treg cells also led to a moderate reduction of blood bacterial load in TNFR2$^{-/-}$ mice (Figure S5B), suggesting ameliorated breaching of the mucosal barrier. Collectively, our data reveal a specific suppression of γδT17 cells by TNFR2$^+$ Treg cells in pneumococcus-infected lungs.

IL-17A blockade prevents the development of bacteremic pneumococcal pneumonia in TNFR2$^{-/-}$ mice

To determine whether overactivated IL-17A expression by γδ T cells in TNFR2$^{-/-}$ mice mediated excessive neutrophil influx into the lung and thereby promoted bacterial dissemination upon pneumococcal infection, mice were administered i.n. with two doses of IL-17A neutralizing antibody at 0 and 6 h post pneumococcal infection, and airway cell infiltration was analyzed at 18 h post infection. A significantly lower number of neutrophils was detected in the airways of mice treated with anti-IL-17A compared with the isotype control group (Figure 6A). Bacterial clearance in the airway and lung tissue was not affected by IL-17A blockade (Figure 6B). Importantly however, anti-IL-17A treatment led to reduced dissemination of bacteria into blood (Figure 6C), correlating with reduced neutrophil infiltration in the lung of TNFR2$^{-/-}$ mice. In correspondence with the lower bacterial load in the blood, blocking IL-17A in the early stages of pneumococcal infection also improved the survival of susceptible TNFR2$^{-/-}$ mice (Figure 6D). Our results indicate that overactivation of IL-17A responses in TNFR2$^{-/-}$ mice underlies their susceptibility to invasive pneumococcal infection.

DISCUSSION

We reveal that TNFR2 signaling is essential for Treg cell-mediated protection against bacteremic pneumococcal pneumonia by controlling IL-17A-producing γδT17 response and neutrophil recruitment in the lung. The activation of γδT17 cells in the lung was found to be negatively regulated by TNFR2$^+$ Treg cells, preventing excessive neutrophilic influx and tissue damaging. This TNFR2-mediated immune regulatory pathway may be one of the key mechanisms to preventing invasive pulmonary infection by opportunistic bacterial pathogens such as *Streptococcus pneumoniae*.

Anti-TNFα therapy, by blocking TNFα signals via both TNFR1 and TNFR2, has been found to increase the risk of severe bacterial infection, and pneumococcus is a recognized causative pathogen for therapy-related pneumonia and bacteremia.[29,37] This increased susceptibility to invasive pneumococcal infection in the absence of TNFα signaling was also evidenced in murine studies.[19,20,38,39] Inhibiting TNFα could lead to neutropenia, which was thought to impair bacteria clearance in pneumococcal infection. However, the lack of TNFα signal did not appear to diminish neutrophil recruitment to the lung in mice challenged with pneumococcus.[20,40] Pulmonary neutrophil recruitment was impaired only when TNFα receptors (both TNFR1 and TNFR2) and the IL-1 receptor (IL-1R1) were collectively deficient.[40] Therefore, it is unlikely that anti-TNFα treatment has led to a higher incidence of invasive pneumococcal disease through dampening the neutrophil response alone. In contrast, we found that in TNFR2-deficient mice, pneumococcal infection-induced neutrophil influx to the lung was enhanced, associated with a marked increase of γδ T cells polarized for IL-17A production, suggesting a lack of suppressive immune responses in the absence of the TNFα-TNFR2 axis. Indeed, TNFR2 deficiency led to reduced numbers of pulmonary Treg cells during pneumococcal infection, predisposing the mice to the development of fatal sepsis.

In response to various inflammatory cues, such as IL-33 in airway hypersensitivity[41] and TNFα in autoimmune conditions,[25,26] Treg cells are activated to keep inflammatory responses under control. TNFα has been shown to activate Treg cells and maintain their stability through TNFR2,[23,25] which can be seen as a negative feedback loop to balance out its potent pro-inflammatory effects, mediated mainly by TNFR1.[42] In the lung, TNFα can be produced by pulmonary macrophages, alveolar epithelial cells, etc., with a detectable background level of expression in the macrophages during homeostasis.[20] Upon pneumococcal infection, TNFα is one of the early response cytokines that is rapidly upregulated, and this coincides with TNFR2-associated Treg cell activation (Figures 2A–2D). Moreover, the

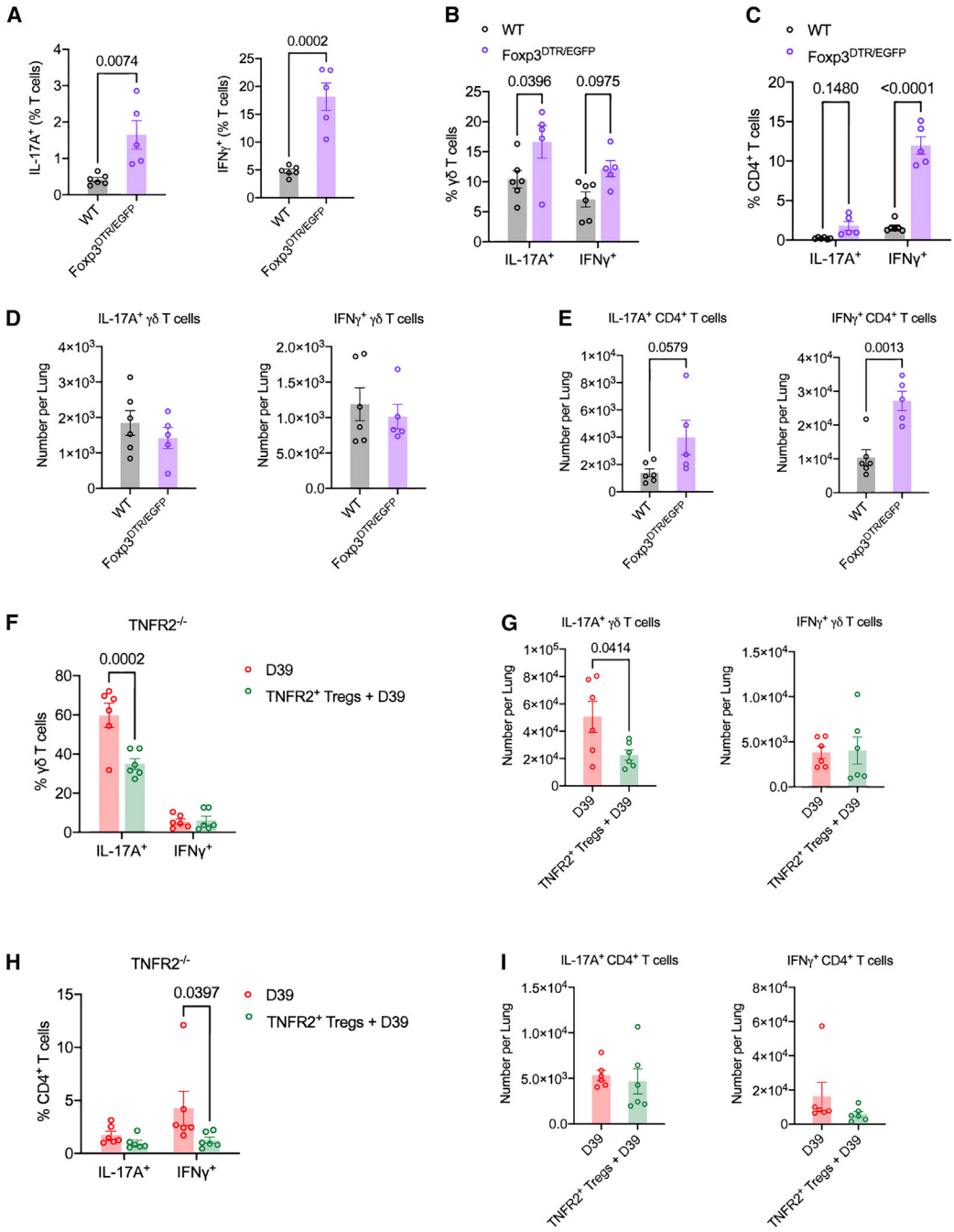

Figure 5. TNFR2$^+$ Treg cells suppress γδT17 cells in pneumococcus-infected lungs

(A–E) Foxp3$^{DTR/EGFP}$ mice and their WT littermates were infected (i.n.) with D39 pneumococci. T cell responses in the lung were analyzed at 18 h p.i.

(A) Proportion of T cells expressing IL-17A or IFNγ.

(B and C) Proportion of IL-17A$^+$ and IFNγ$^+$ cells in γδ (B) and CD4$^+$ (C) T cells, respectively.

(D) Number of IL-17A and IFNγ-producing γδ T cells.

(E) Number of IL-17A and IFNγ-producing CD4$^+$ T cells. Data represent one (n = 5 mice per group) of two independent experiments.

(F–I) TNFR2$^{-/-}$ mice were i.v. injected with 2 × 10^5 of TNFR2$^+$ Treg cells or PBS for the control group and then infected (i.n.) with D39 pneumococci at 24 h post the adoptive transfer. Lung T cell responses were analyzed at 18 h p.i.

(F and G) Proportion (F) and number (G) of IL-17A$^+$ and IFNγ$^+$ cells in γδ T cells.

(H and I) Proportion (H) and number (I) of IL-17A$^+$ and IFNγ$^+$ cells in CD4$^+$ T cells. Data were pooled of two independent experiments (n = 6 mice per group). Unpaired two-tailed t test was used to analyze data in (A), (D), (E), (G), and (I). Data in (B), (C), (F), and (H) were analyzed by ordinary two-way ANOVA with Sidak's multiple comparisons test.

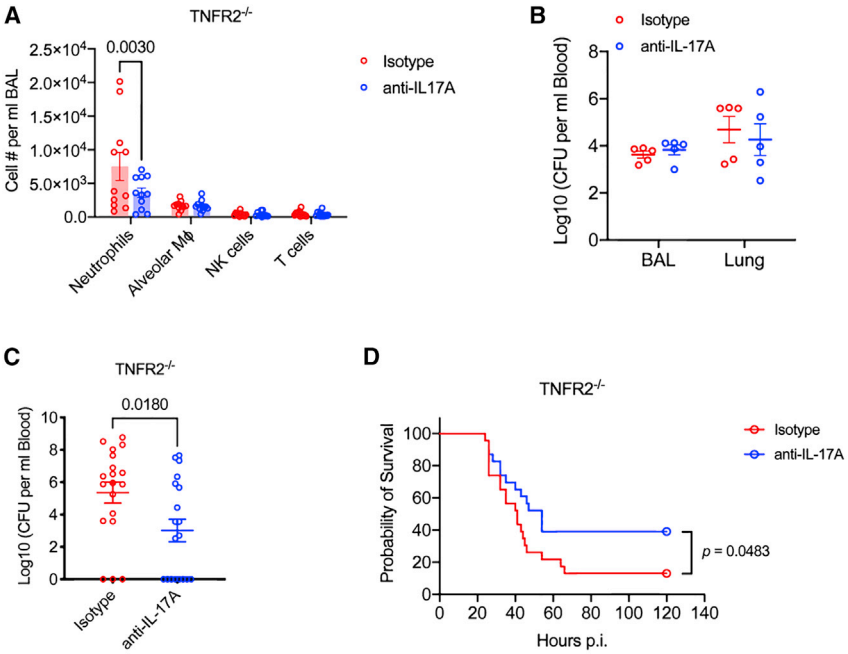

Figure 6. IL-17A blockade prevents the development of bacteremic pneumococcal pneumonia in TNFR2$^{-/-}$ mice

(A–D) TNFR2$^{-/-}$ mice were treated (i.n.) with anti-IL-17A monoclonal antibody or isotype control at 0 and 6 h post i.n. infection of D39 pneumococci. Infected mice were analyzed at 18 h p.i. for data in (A)–(C).

(A) Number of neutrophils, alveolar Mφ, NK cells, and T cells in the BAL. Data were pooled from two independent experiments (n = 11 mice per group).

(B) Bacterial count in the BAL and lung homogenates. Data represent one (n = 5 mice per group) of two independent experiments.

(C) Bacterial count in the blood. Data were pooled from three independent experiments (n = 19 mice per group). Unpaired two-tailed t test was used to analyze the data.

(D) Survival of infected mice. Data were pooled from four independent experiments (n = 23 mice per group) and analyzed using Log rank (Mantel-Cox) test. Ordinary two-way ANOVA with Sidak's multiple comparisons test was used for the statistical analysis in (A) and (B).

lung parenchymal T cell population is composed of a significantly higher proportion of TNFR2^{+} Treg cells, as compared with the T cell populations in lung vasculature and spleen (unpublished data). Since the short time frame precludes development of antigen-specific T cell responses during acute pneumococcal pneumonia, the activation of pulmonary TNFR2^{+} Treg cells is likely via a T cell receptor (TCR)-independent mechanism but requires TNF signals. In the lung of TNFR2-deficient mice, Treg cells could still acquire effector phenotype following pneumococcal infection, indicating that the TNFα-TNFR2 axis is not an absolute requirement for Treg activation. However, the frequency and number of Treg cells dropped significantly in the absence of TNFR2 (Figure 2), which is consistent with the critical role of TNFR2 that has been demonstrated in inflammatory bowel disease, where it was found to stabilize the Treg cell population at the site of inflammation.[25] The monoclonal antibody or receptor fusion protein used in anti-TNFα therapy blocks TNF, without discriminating signaling through TNFR1 and TNFR2, it can therefore lead to a deficiency in TNFR2-mediated Treg cell maintenance and suppressive function, which is pivotal to control pro-inflammatory responses elicited by a range of stimuli.[27] In pneumococcal infection, TNFR2 deficiency removed TNFR2^{+} Treg cell-mediated suppression on γδT17 response, contributing to augmented neutrophilic inflammation in the lung.

Apart from Treg cells, TNFR2 is also shown to regulate macrophage polarization, which may also contribute to the control of inflammation.[43] However, TNFR2 expression was detected in pulmonary NK cells but not in alveolar macrophages (Figure S6). Along with enhanced neutrophil infiltration, TNFR2$^{-/-}$ mice also had a small, but significant, increase of NK cells in the lung following pneumococcal infection, suggesting that TNFR2 may directly suppress NK cell recruitment. We cannot conclude though whether this small increase of NK cells affects the γδT17 response in pneumococcus-infected lungs, but the number of NK cells was not affected by IL-17A blockade (Figure 6A), suggesting that their recruitment/migration is less relevant to the TNFR2+ Treg cell-γδT17 axis in the lung.

IL-17A is a critical inflammatory cytokine that induces neutrophil infiltration in various inflammatory settings.[14,15,34] γδ T cells are the major source of IL-17A responding to pneumococcal infection.[36] Deficiency in IL-17A or γδ T cells has been reported to impair the neutrophil response during pneumococcal pneumonia, causing increased bacterial load locally and systemically.[36,44] A suppressed IL-17A response post influenza virus infection has been shown to make mice more susceptible to a secondary pneumococcal infection.[45] Although most studies have focused on IL-17A and γδ T cell-mediated host defense to pneumococcus and tried to foster strategies to boost γδT17 response, the potentially deleterious effects of overactivation of these cells have not received sufficient consideration. Here, we have demonstrated that γδT17 cells increase dramatically in the lung of TNFR2-deficient mice, with over 75% of IL-17A^{+} T cells being γδ T cells after pneumococcal infection. As expected, this led to enhanced neutrophil recruitment into the airway. However, such robust activation of the IL-17A-neutrophil axis did not accelerate bacterial clearance in the airway but instead resulted in a significantly increased bacteria load in the blood leading to shortened survival time and reduced survival rate. Our results clearly demonstrate how uncontrolled activation of γδT17 responses are highly detrimental during invasive pneumococcal infection.

Furthermore, we found that TNFR2$^{-/-}$ mice, which lack TNFR2^{+} Treg cells, were more susceptible to pneumococcal infection than DEREG mice depleted of total Treg cell population, as indicated by a more pronounced blood dissemination of bacteria and shorter median survival time in TNFR2$^{-/-}$ animals. Intracellular cytokine

staining showed that total Treg cell depletion promoted both IL-17 and IFNγ expression in γδ and $CD4^+$ T cells, while in the absence of $TNFR2^+$ Treg cells, a subpopulation of Treg cells, the enhancement of IL-17A expression in γδ T cells was of a greater magnitude, but the IFNγ responses were unaffected. This further highlights the deleterious effect caused by overactivation of γδT17 cells in pneumococcal pneumonia. It has been demonstrated that IFNγ is able to suppress Th17 induction and IFNγ blockade can enhance IL-17A expression by $CD4^+$ T cells,[46,47] findings that may provide an explanation for our observations in infected DEREG mice. Similar to Th17 cells, activation of γδT17 requires signals from the STAT3 transcription factor,[48] hence it is possible that IFNγ can negatively regulate γδT17 response by inducing STAT1-mediated inhibition on STAT3.[49]

Treg cells regulate inflammatory T cell responses through several mechanisms, including those driven by TGF-β and IL-10. However, these two cytokines are known to strongly suppress IFNγ responses, whereas the suppression of γδT17 by $TNFR2^+$ Treg cells that we observed here was specific and did not similarly inhibit the Th1 or IFNγ response. Rather, a more recently identified Treg cytokine, IL-35, may have contributed to this discriminated regulation of the IL-17 response. We and others have shown that IL-35 has the ability to specifically suppress IL-17A responses in both murine and human T cells.[50,51] IL-35 has also been shown to suppress γδ T cell IL-17 responses in the lung during allergic inflammation.[41] Our early efforts to examine IL-35 expression by pulmonary Treg cells using intracellular cytokine staining have been inconclusive, but this remains a priority for future study. Another key area for follow-up is the potential for feedback regulation of Treg responses via γδ T cell-derived TNFα. We found that a large proportion of IL-17A-expressing γδ T cells also co-express TNFα (Figure S7). Hence, it is possible that this may also promote $TNFR2^+$ Treg cell-mediated suppression.

Taken together, our results demonstrate that uncontrolled, excessive neutrophil infiltration into lungs during pneumococcal pneumonia is associated with increased risk of systemic bacterial invasion. $TNFR2^+$ Treg cells regulate the activation of pulmonary γδT17 cells, thereby controlling neutrophilic influx and associated inflammation in pneumococcus-infected lungs. TNFR2-mediated Treg responses may be the key to preventing overactivation of inflammatory responses in respiratory infections and other inflammatory diseases. Further investigation to clarify the functional mechanism of pulmonary $TNFR2^+$ Treg cells is warranted, to identify potential molecular targets against invasive pneumococcal disease. Any future interventions targeting the $TNFR2^+$ Treg- γδT17 axis would need to be fast-acting, given the importance of this immune crosstalk during the early stages of acute infection.

Limitations of the study

In this study, we show that TNFR2 deficiency impairs the maintenance and function of pulmonary Treg cells, leading to increased susceptibility to pneumococcal infection. Some limitations of our study may include the potential influence of other TNFR2-expressing immune cells and whether depletion of $TNFR2^+$ Treg cells systemically would have any significant effect. Also, in our study we focused on male mice given the well-established higher incidence of pneumococcal disease in males, and although TNFR2 deficiency did affect male mice more significantly during pneumococcal pneumonia, its role in females should be addressed more specifically in following studies, given the large proportion of female patients with rheumatoid arthritis that may be offered anti-TNF therapy.

STAR★METHODS

Detailed methods are provided in the online version of this paper and include the following:

- KEY RESOURCES TABLE
- RESOURCE AVAILABILITY
  - Lead contact
  - Materials availability
  - Data and code availability
- EXPERIMENTAL MODEL AND SUBJECT DETAILS
  - Mice
  - Bacteria
- METHOD DETAILS
  - Mouse model of pneumococcal pneumonia
  - Treg cell depletion in DEREG mice
  - IL-17A blockade in $TNFR2^{-/-}$ mice
  - $TNFR2^+$ Treg cell sorting and adoptive transfer
  - Lung tissue processing
  - Quantification of pneumococcus
  - Flow cytometry
  - Lung T cell isolation and RT-qPCR
  - Histology
- QUANTIFICATION AND STATISTICAL ANALYSIS

SUPPLEMENTAL INFORMATION

Supplemental information can be found online at https://doi.org/10.1016/j.celrep.2023.112054.

ACKNOWLEDGMENTS

The study was funded by UK Medical Research Council Programme grant (MR/P011284/1).

AUTHOR CONTRIBUTIONS

R.X., L.C.J., D.R.N., and A.K. conceived and designed the experiments; R.X., L.C.J., S.K., D.B., and M.L.R. performed the experiments; R.X., L.C.J., X.Q.W., N.F., D.R.N., and A.K. analyzed the data; R.X. drafted and revised the manuscript; X.Q.W., N.F., D.R.N., and A.K. edited and revised the manuscript; A.K. supervised the study. All authors read and approved the final version of the manuscript.

DECLARATION OF INTERESTS

A.K. is the founder of ReNewVax Ltd and a member of its scientific advisory board.

Received: May 9, 2022
Revised: December 9, 2022
Accepted: January 17, 2023

REFERENCES

1. Nathan, C. (2002). Points of control in inflammation. Nature *420*, 846–852. https://doi.org/10.1038/nature01320.
2. Ribet, D., and Cossart, P. (2015). How bacterial pathogens colonize their hosts and invade deeper tissues. Microbes Infect. *17*, 173–183. https://doi.org/10.1016/j.micinf.2015.01.004.
3. Kadioglu, A., Weiser, J.N., Paton, J.C., and Andrew, P.W. (2008). The role of Streptococcus pneumoniae virulence factors in host respiratory colonization and disease. Nat. Rev. Microbiol. *6*, 288–301. https://doi.org/10.1038/nrmicro1871.
4. Said, M.A., Johnson, H.L., Nonyane, B.A.S., Deloria-Knoll, M., and O'Brien, K.L.; AGEDD Adult Pneumococcal Burden Study Team (2013). Estimating the burden of pneumococcal pneumonia among adults: a systematic review and meta-analysis of diagnostic techniques. PLoS One *8*, e60273. https://doi.org/10.1371/journal.pone.0060273.
5. Bordon, J.M., Fernandez-Botran, R., Wiemken, T.L., Peyrani, P., Uriarte, S.M., Arnold, F.W., Rodriquez-Hernandez, L., Rane, M.J., Kelley, R.R., Binford, L.E., et al. (2015). Bacteremic pneumococcal pneumonia: clinical outcomes and preliminary results of inflammatory response. Infection *43*, 729–738. https://doi.org/10.1007/s15010-015-0837-z.
6. Lin, S.H., Lai, C.C., Tan, C.K., Liao, W.H., and Hsueh, P.R. (2011). Outcomes of hospitalized patients with bacteraemic and non-bacteraemic community-acquired pneumonia caused by *Streptococcus pneumoniae*. Epidemiol. Infect. *139*, 1307–1316. https://doi.org/10.1017/s0950268810002402.
7. Herbold, W., Maus, R., Hahn, I., Ding, N., Srivastava, M., Christman, J.W., Mack, M., Reutershan, J., Briles, D.E., Paton, J.C., et al. (2010). Importance of CXC chemokine receptor 2 in alveolar neutrophil and exudate macrophage recruitment in response to pneumococcal lung infection. Infect. Immun. *78*, 2620–2630. https://doi.org/10.1128/iai.01169-09.
8. Lee, W.L., and Downey, G.P. (2001). Neutrophil activation and acute lung injury. Curr. Opin. Crit. Care *7*, 1–7. https://doi.org/10.1097/00075198-200102000-00001.
9. José, R.J., Williams, A.E., Mercer, P.F., Sulikowski, M.G., Brown, J.S., and Chambers, R.C. (2015). Regulation of neutrophilic inflammation by proteinase-activated receptor 1 during bacterial pulmonary infection. J. Immunol. *194*, 6024–6034. https://doi.org/10.4049/jimmunol.1500124.
10. Gierlikowska, B., Stachura, A., Gierlikowski, W., and Demkow, U. (2021). Phagocytosis, degranulation and extracellular traps release by neutrophils—the current knowledge, pharmacological modulation and future prospects. Front. Pharmacol. *12*, 666732. https://doi.org/10.3389/fphar.2021.666732.
11. Sabbaghi, A., Miri, S.M., Keshavarz, M., Mahooti, M., Zebardast, A., and Ghaemi, A. (2020). Role of γδ T cells in controlling viral infections with a focus on influenza virus: implications for designing novel therapeutic approaches. Virol. J. *17*, 174. https://doi.org/10.1186/s12985-020-01449-0.
12. Ivanov, S., Paget, C., and Trottein, F. (2014). Role of non-conventional T lymphocytes in respiratory infections: the case of the pneumococcus. PLoS Pathog. *10*, e1004300. https://doi.org/10.1371/journal.ppat.1004300.
13. Kirby, A.C., Newton, D.J., Carding, S.R., and Kaye, P.M. (2007). Evidence for the involvement of lung-specific gammadelta T cell subsets in local responses to Streptococcus pneumoniae infection. Eur. J. Immunol. *37*, 3404–3413. https://doi.org/10.1002/eji.200737216.
14. Cai, Y., Shen, X., Ding, C., Qi, C., Li, K., Li, X., Jala, V.R., Zhang, H.g., Wang, T., Zheng, J., et al. (2011). Pivotal role of dermal IL-17-producing γδ T cells in skin inflammation. Immunity *35*, 596–610. https://doi.org/10.1016/j.immuni.2011.08.001.
15. Coffelt, S.B., Kersten, K., Doornebal, C.W., Weiden, J., Vrijland, K., Hau, C.-S., Verstegen, N.J.M., Ciampricotti, M., Hawinkels, L.J.A.C., Jonkers, J., and De Visser, K.E. (2015). IL-17-producing γδ T cells and neutrophils conspire to promote breast cancer metastasis. Nature *522*, 345–348. https://doi.org/10.1038/nature14282.
16. Hong, M.J., Gu, B.H., Madison, M.C., Landers, C., Tung, H.Y., Kim, M., Yuan, X., You, R., Machado, A.A., Gilbert, B.E., et al. (2018). Protective role of γδ T cells in cigarette smoke and influenza infection. Mucosal Immunol. *11*, 894–908. https://doi.org/10.1038/mi.2017.93.
17. Neill, D.R., Fernandes, V.E., Wisby, L., Haynes, A.R., Ferreira, D.M., Laher, A., Strickland, N., Gordon, S.B., Denny, P., Kadioglu, A., and Andrew, P.W. (2012). T regulatory cells control susceptibility to invasive pneumococcal pneumonia in mice. PLoS Pathog. *8*, e1002660. https://doi.org/10.1371/journal.ppat.1002660.
18. Xiong, Y., Zhong, Q., Palmer, T., Benner, A., Wang, L., Suresh, K., Damico, R., and D'Alessio, F.R. (2021). Estradiol resolves pneumonia via ERβ in regulatory T cells. JCI Insight *6*, e133251. https://doi.org/10.1172/jci.insight.133251.
19. Takashima, K., Tateda, K., Matsumoto, T., Iizawa, Y., Nakao, M., and Yamaguchi, K. (1997). Role of tumor necrosis factor alpha in pathogenesis of pneumococcal pneumonia in mice. Infect. Immun. *65*, 257–260. https://doi.org/10.1128/iai.65.1.257-260.1997.
20. Kirby, A.C., Raynes, J.G., and Kaye, P.M. (2005). The role played by tumor necrosis factor during localized and systemic infection withStreptococcus pneumoniae. J. Infect. Dis. *191*, 1538–1547. https://doi.org/10.1086/429296.
21. Kerr, A.R., Irvine, J.J., Search, J.J., Gingles, N.A., Kadioglu, A., Andrew, P.W., McPheat, W.L., Booth, C.G., and Mitchell, T.J. (2002). Role of inflammatory mediators in resistance and susceptibility to pneumococcal infection. Infect. Immun. *70*, 1547–1557. https://doi.org/10.1128/iai.70.3.1547-1557.2002.
22. Chen, X., Bäumel, M., Männel, D.N., Howard, O.M.Z., and Oppenheim, J.J. (2007). Interaction of TNF with TNF receptor type 2 promotes expansion and function of mouse CD4+CD25+ T regulatory cells. J. Immunol. *179*, 154–161. https://doi.org/10.4049/jimmunol.179.1.154.
23. Chen, X., and Oppenheim, J.J. (2010). TNF-α: an activator of CD4+FoxP3+TNFR2+ regulatory T cells. Curr. Dir. Autoimmun., 119–134. https://doi.org/10.1159/000289201.
24. Fischer, R., Kontermann, R.E., and Pfizenmaier, K. (2020). Selective targeting of TNF receptors as a novel therapeutic approach. Front. Cell Dev. Biol. *8*, 401. https://doi.org/10.3389/fcell.2020.00401.
25. Chen, X., Wu, X., Zhou, Q., Howard, O.M.Z., Netea, M.G., and Oppenheim, J.J. (2013). TNFR2 is critical for the stabilization of the CD4+Foxp3+ regulatory T. cell phenotype in the inflammatory environment. J. Immunol. *190*, 1076–1084. https://doi.org/10.4049/jimmunol.1202659.
26. Atretkhany, K.S.N., Mufazalov, I.A., Dunst, J., Kuchmiy, A., Gogoleva, V.S., Andruszewski, D., Drutskaya, M.S., Faustman, D.L., Schwabenland, M., Prinz, M., et al. (2018). Intrinsic TNFR2 signaling in T regulatory cells provides protection in CNS autoimmunity. Proc. Natl. Acad. Sci. USA *115*, 13051–13056. https://doi.org/10.1073/pnas.1807499115.
27. Yang, S., Wang, J., Brand, D.D., and Zheng, S.G. (2018). Role of TNF–TNF receptor 2 signal in regulatory T cells and its therapeutic implications. Front. Immunol. *9*, 784. https://doi.org/10.3389/fimmu.2018.00784.
28. Baghai, M., Osmon, D.R., Wolk, D.M., Wold, L.E., Haidukewych, G.J., and Matteson, E.L. (2001). Fatal sepsis in a patient with rheumatoid arthritis treated with etanercept. Mayo Clin. Proc. *76*, 653–656. https://doi.org/10.4065/76.6.653.
29. Wright, S.A., and Taggart, A.J. (2004). Pneumococcal vaccination for RA patients on TNF- antagonists. Rheumatology *43*, 523. https://doi.org/10.1093/rheumatology/keh167.
30. Uthman, I., Husari, A., Touma, Z., and Kanj, S.S. (2005). Fatal streptococcal toxic shock syndrome in a patient with rheumatoid arthritis treated with etanercept. Rheumatology *44*, 1200–1201. https://doi.org/10.1093/rheumatology/keh680.
31. Nuñez-Cornejo, C., Borrás-Blasco, J., Gracia-Perez, A., Rosique-Robles, J.D., Lopez-Camps, V., Casterã, E., and Abad, F.J. (2008). Septic shock and community-acquired pneumonia associated with etanercept therapy.

Int. J. Clin. Pharmacol. Ther. *46*, 193–197. https://doi.org/10.5414/cpp46193.

32. Gerberick, G.F., Cruse, L.W., Miller, C.M., Sikorski, E.E., and Ridder, G.M. (1997). Selective modulation of T cell memory markers CD62L and CD44 on murine draining lymph node cells following allergen and irritant treatment. Toxicol. Appl. Pharmacol. *146*, 1–10. https://doi.org/10.1006/taap.1997.8218.

33. Lahl, K., and Sparwasser, T. (2011). In Vivo Depletion of FoxP3+ Tregs Using the DEREG Mouse Model (Humana Press), pp. 157–172. https://doi.org/10.1007/978-1-61737-979-6_10.

34. Schwarzenberger, P., Huang, W., Ye, P., Oliver, P., Manuel, M., Zhang, Z., Bagby, G., Nelson, S., and Kolls, J.K. (2000). Requirement of endogenous stem cell factor and granulocyte-colony-stimulating factor for IL-17-mediated granulopoiesis. J. Immunol. *164*, 4783–4789. https://doi.org/10.4049/jimmunol.164.9.4783.

35. Hassane, M., Jouan, Y., Creusat, F., Soulard, D., Boisseau, C., Gonzalez, L., Patin, E.C., Heuzé-Vourc'h, N., Sirard, J.-C., Faveeuw, C., et al. (2020). Interleukin-7 protects against bacterial respiratory infection by promoting IL-17A-producing innate T-cell response. Mucosal Immunol. *13*, 128–139. https://doi.org/10.1038/s41385-019-0212-y.

36. Hassane, M., Demon, D., Soulard, D., Fontaine, J., Keller, L.E., Patin, E.C., Porte, R., Prinz, I., Ryffel, B., Kadioglu, A., et al. (2017). Neutrophilic NLRP3 inflammasome-dependent IL-1beta secretion regulates the gammadeltaT17 cell response in respiratory bacterial infections. Mucosal Immunol. *10*, 1056–1068. https://doi.org/10.1038/mi.2016.113.

37. Kroesen, S., Widmer, A.F., Tyndall, A., and Hasler, P. (2003). Serious bacterial infections in patients with rheumatoid arthritis under anti-TNF-alpha therapy. Rheumatology *42*, 617–621. https://doi.org/10.1093/rheumatology/keg263.

38. van der Poll, T., Keogh, C.V., Buurman, W.A., and Lowry, S.F. (1997). Passive immunization against tumor necrosis factor-alpha impairs host defense during pneumococcal pneumonia in mice. Am. J. Respir. Crit. Care Med. *155*, 603–608. https://doi.org/10.1164/ajrccm.155.2.9032201.

39. Rijneveld, A.W., Florquin, S., Branger, J., Speelman, P., Van Deventer, S.J., and Van Der Poll, T. (2001). TNF-α compensates for the impaired host defense of IL-1 type I receptor-deficient mice during pneumococcal pneumonia. J. Immunol. *167*, 5240–5246. https://doi.org/10.4049/jimmunol.167.9.5240.

40. Jones, M.R., Simms, B.T., Lupa, M.M., Kogan, M.S., and Mizgerd, J.P. (2005). Lung NF-κB activation and neutrophil recruitment require IL-1 and TNF receptor signaling during pneumococcal pneumonia. J. Immunol. *175*, 7530–7535. https://doi.org/10.4049/jimmunol.175.11.7530.

41. Faustino, L.D., Griffith, J.W., Rahimi, R.A., Nepal, K., Hamilos, D.L., Cho, J.L., Medoff, B.D., Moon, J.J., Vignali, D.A.A., and Luster, A.D. (2020). Interleukin-33 activates regulatory T cells to suppress innate $\gamma\delta$ T cell responses in the lung. Nat. Immunol. *21*, 1371–1383. https://doi.org/10.1038/s41590-020-0785-3.

42. Peschon, J.J., Torrance, D.S., Stocking, K.L., Glaccum, M.B., Otten, C., Willis, C.R., Charrier, K., Morrissey, P.J., Ware, C.B., and Mohler, K.M. (1998). TNF receptor-deficient mice reveal divergent roles for p55 and p75 in several models of inflammation. J. Immunol. *160*, 943–952.

43. Fu, W., Hu, W., Yi, Y.S., Hettinghouse, A., Sun, G., Bi, Y., He, W., Zhang, L., Gao, G., Liu, J., et al. (2021). TNFR2/14-3-3epsilon signaling complex instructs macrophage plasticity in inflammation and autoimmunity. J. Clin. Invest. *131*, e144016. https://doi.org/10.1172/JCI144016.

44. Nakasone, C., Yamamoto, N., Nakamatsu, M., Kinjo, T., Miyagi, K., Uezu, K., Nakamura, K., Higa, F., Ishikawa, H., O'Brien, R.L., et al. (2007). Accumulation of gamma/delta T cells in the lungs and their roles in neutrophil-mediated host defense against pneumococcal infection. Microbes Infect. *9*, 251–258. https://doi.org/10.1016/j.micinf.2006.11.015.

45. Li, W., Moltedo, B., and Moran, T.M. (2012). Type I interferon induction during influenza virus infection increases susceptibility to secondary Streptococcus pneumoniae infection by negative regulation of T cells. J. Virol. *86*, 12304–12312. https://doi.org/10.1128/jvi.01269-12.

46. Evans, H.G., Suddason, T., Jackson, I., Taams, L.S., and Lord, G.M. (2007). Optimal induction of T helper 17 cells in humans requires T cell receptor ligation in the context of Toll-like receptor-activated monocytes. Proc. Natl. Acad. Sci. USA *104*, 17034–17039. https://doi.org/10.1073/pnas.0708426104.

47. Harrington, L.E., Hatton, R.D., Mangan, P.R., Turner, H., Murphy, T.L., Murphy, K.M., and Weaver, C.T. (2005). Interleukin 17–producing CD4+ effector T cells develop via a lineage distinct from the T helper type 1 and 2 lineages. Nat. Immunol. *6*, 1123–1132. https://doi.org/10.1038/ni1254.

48. Agerholm, R., Rizk, J., Viñals, M.T., and Bekiaris, V. (2019). STAT 3 but not STAT 4 is critical for $\gamma\delta$T17 cell responses and skin inflammation. EMBO Rep. *20*, e48647. https://doi.org/10.15252/embr.201948647.

49. Hiller, J., Hagl, B., Effner, R., Puel, A., Schaller, M., Mascher, B., Eyerich, S., Eyerich, K., Jansson, A.F., Ring, J., et al. (2018). STAT1 gain-of-function and dominant negative STAT3 mutations impair IL-17 and IL-22 immunity associated with CMC. J. Invest. Dermatol. *138*, 711–714. https://doi.org/10.1016/j.jid.2017.09.035.

50. Xu, R., Shears, R.K., Sharma, R., Krishna, M., Webb, C., Ali, R., Wei, X., Kadioglu, A., and Zhang, Q. (2020). IL-35 is critical in suppressing superantigenic Staphylococcus aureus-driven inflammatory Th17 responses in human nasopharynx-associated lymphoid tissue. Mucosal Immunol. *13*, 460–470. https://doi.org/10.1038/s41385-019-0246-1.

51. Niedbala, W., Wei, X.-Q., Cai, B., Hueber, A.J., Leung, B.P., McInnes, I.B., and Liew, F.Y. (2007). IL-35 is a novel cytokine with therapeutic effects against collagen-induced arthritis through the expansion of regulatory T cells and suppression of Th17 cells. Eur. J. Immunol. *37*, 3021–3029. https://doi.org/10.1002/eji.200737810.

52. Jacques, L.C., Green, A.E., Barton, T.E., Baltazar, M., Aleksandrowicz, J., Xu, R., Trochu, E., Kadioglu, A., and Neill, D.R. (2022). Influence of Streptococcus pneumoniae within-strain population diversity on virulence and pathogenesis. Microbiol. Spectr., e0310322. https://doi.org/10.1128/spectrum.03103-22.

53. Bankhead, P., Loughrey, M.B., Fernández, J.A., Dombrowski, Y., McArt, D.G., Dunne, P.D., McQuaid, S., Gray, R.T., Murray, L.J., Coleman, H.G., et al. (2017). QuPath: open source software for digital pathology image analysis. Sci. Rep. *7*, 16878. https://doi.org/10.1038/s41598-017-17204-5.

54. Kadioglu, A., Gingles, N.A., Grattan, K., Kerr, A., Mitchell, T.J., and Andrew, P.W. (2000). Host cellular immune response to pneumococcal lung infection in mice. Infect. Immun. *68*, 492–501. https://doi.org/10.1128/iai.68.2.492-501.2000.

55. Morton, D.B., and Griffiths, P.H. (1985). Guidelines on the recognition of pain, distress and discomfort in experimental animals and an hypothesis for assessment. Vet. Rec. *116*, 431–436. https://doi.org/10.1136/vr.116.16.431.

56. Van Hoecke, L., Job, E.R., Saelens, X., and Roose, K. (2017). Bronchoalveolar lavage of murine lungs to analyze inflammatory cell infiltration. J. Vis. Exp., 55398. https://doi.org/10.3791/55398.

57. Lim, J.F., Berger, H., and Su, I.H. (2016). Isolation and activation of murine lymphocytes. J. Vis. Exp., 54596. https://doi.org/10.3791/54596.

STAR★METHODS

KEY RESOURCES TABLE

REAGENT or RESOURCE	SOURCE	IDENTIFIER
Antibodies		
*InVivo*MAb anti-mouse IL-17A	BioXCell	Clone 17F3; Cat#BE0173
*InVivo*MAb mouse IgG1 isotype control	BioXCell	Clone MOPC-21; Cat#BE0083
Anti-mouse CD25-PE	Miltenyi Biotec	Clone 7D4; Cat#130-118-550; RRID:AB_2784088
Anti-mouse TNFR2-APC	Miltenyi Biotec	Clone REA228; Cat#130-123-275; RRID:AB_2889435
Anti-mouse CD127-BV421	BioLegend	Clone A7R34; Cat#135027; RRID:AB_2563103
Anti-mouse CD45-PE-Cy7	BioLegend	Clone 30-F11; Cat#103114; RRID:AB_312979
Anti-mouse CD3-FITC	BioLegend	Clone 17A2; Cat#100204; RRID:AB_312661
Anti-mouse/human CD11b-PE	BioLegend	Clone M1/70; Cat#101208; RRID:AB_312791
Anti-mouse Ly6G-APC-Cy7	BioLegend	Clone 1A8; Cat#127624; RRID:AB_10640819
Anti-mouse NKp46-APC	BioLegend	Clone 29A1.4; Cat#137608; RRID:AB_10612758
Anti-mouse CD3-APC	BioLegend	Clone 17A2; Cat#100236; RRID:AB_2561456
Anti-mouse CD4-APC-Cy7	BioLegend	Clone GK1.5; Cat#100414; RRID:AB_312699
Anti-mouse TCR$\gamma\delta$-PE-Cy7	BioLegend	Clone GL3; Cat#118124; RRID:AB_11204423
Anti-mouse IL-17A-PE	BioLegend	Clone TC11-18H10.1; Cat#506904; RRID:AB_315464
Anti-mouse IFNγ-BV421	BioLegend	Clone XMG1.2; Cat#505830; RRID:AB_2563105
Anti-mouse CD3-PE-Cy7	BioLegend	Clone 17A2; Cat#100220; RRID:AB_1732057
Anti-mouse TNFR2-PE	BioLegend	Clone TR75-89; Cat#113406; RRID:AB_2206941
Anti-mouse/human CD44-APC	BioLegend	Clone IM7; Cat#103012; RRID:AB_312963
Anti-mouse CD62L-Pacific Blue	BioLegend	Clone MEL-14; Cat#104424; RRID:AB_493380
Anti-mouse Foxp3-Alexa Fluor 488	BioLegend	Clone MF-14; Cat#126406; RRID:AB_1089113
Anti-mouse SiglecF-BV421	BD Biosciences	Clone E50-2440; Cat#562681; RRID:AB_2722581
Bacterial and virus strains		
Serotype 2 *S pneumoniae* strain D39	Jacques[52]	NCTC7466
Chemicals, peptides, and recombinant proteins		
Diphtheria toxin	Merck	Cat#322326
Cell Activation Cocktail (with Brefeldin A)	BioLegend	Cat#423304
IC Fixation Buffer	Fisher/Invitrogen	Cat#00-8222-49
Foxp3/Transcription Factor Staining Buffer Set	Fisher/Invitrogen	Cat#00-5523-00
Type 1 collagenase	Fisher/Gibco	Cat#17018029
DNase 1	Merck/Sigma Aldrich	Cat#11284932001
True-Stain Monocyte Blocker	BioLegend	Cat#426103
LIVE/DEAD Fixable Aqua Dead Cell Stain Kit	Fisher/Molecular Probes	Cat#L34965
M-MLV reverse transcriptase	Promega	Cat#M1701
SYBR® Green JumpStart™ Taq ReadyMix™	Merck/Sigma Aldrich	Cat#S4438
Critical commercial assays		
CD4$^+$ T cell isolation kit, mouse	Miltenyi Biotec	Cat#130-104-454
Anti-PE Microbeads	Miltenyi Biotec	Cat#130-048-801
CD90.2 Microbeads	Miltenyi Biotec	Cat#130-121-278
eBioscience™ Mouse TNF alpha Ready-SET-Go! Kit	Fisher/Invitrogen	Cat#88-7324-77
RNeasy Mini Kit	Qiagen	Cat#74104

(*Continued on next page*)

Continued

REAGENT or RESOURCE	SOURCE	IDENTIFIER
Experimental models: Organisms/strains		
Mouse: Foxp3$^{DTR/EGFP}$: DEpletion of REGulatory T cells (DEREG)	Lahl[33]	N/A
Mouse: TNFR2$^{-/-}$: B6.129S2-*Tnfrsf1b*^{tm1Mwm}/J	The Jackson Laboratory	RRID: IMSR_JAX:002,620
Oligonucleotides		
Random primers	Promega	Cat#C1181
Primer: *Il17a* Forward: CCAGCTGATCAGGACGCGCAAACATGAG	This paper	N/A
Primer: *Il17a* Reverse: TGAGGGATGATCGCTGCTGCCTTCACTG	This paper	N/A
Primer: *Hprt* Forward: GCAGTCCCAGCGTCGTGATTAGCGATGA	This paper	N/A
Primer: *Hprt* Reverse: CCCCTTGAGCACACAGAGGGCCACAATG	This paper	N/A
Software and algorithms		
FlowJo 10.4	BD	https://www.flowjo.com/
QuPath-0.2.3	Bankhead[53]	https://qupath.github.io/
GraphPad Prism (version 9.0.1)	GraphPad Software	https://www.graphpad.com/scientific-software/prism/

RESOURCE AVAILABILITY

Lead contact

Further information and requests for resources and reagents should be directed to and will be fulfilled by the lead contact, Aras Kadioglu (a.kadioglu@liverpool.ac.uk).

Materials availability

This study did not generate new unique reagents.

Data and code availability

- All data reported in this paper will be shared by the lead contact upon request.
- This paper does not report original code.
- Any additional information required to reanalyse the data reported in this paper is available from the lead contact upon request.

EXPERIMENTAL MODEL AND SUBJECT DETAILS

Mice

C57BL/6J (wildtype) mice were purchased from Charles River. Male heterozygous Foxp3$^{DTR/EGFP}$ DEREG mice were kindly provided by Tim Sparwasser (TWINCORE, Hannover) and crossed with female C57BL/6J (wildtype) mice to generate heterozygous Foxp3$^{DTR/EGFP}$ mice and wildtype littermates. B6.129S2-*Tnfrsf1b*^{tm1Mwm}/J (TNFR2$^{-/-}$) mice were purchased from The Jackson Laboratory and bred to generate homozygous knockout mice. All mice used in this study were 7–10 weeks males and age-matched animals were randomly assigned to experimental groups. All mice were bred and maintained in individually ventilated cages at 22 ± 1°C and 65% humidity with a 12hr light-dark cycle. Prior to use, mice were acclimatised for one week with free access to food and water. All experimental protocols were approved and performed in accordance with the regulations of the Home Office Scientific Procedures Act (1986), project licence P86De83DA and the University of Liverpool Ethical and Animal Welfare Committee.

Bacteria

Serotype 2 *S pneumoniae* strain D39 was cultured on blood agar base (BAB) supplemented with 5% (v/v) defibrinated horse blood at 37°C, 5% CO_2. Single colonise were transferred to brain heart infusion broth supplemented with 20% (v/v) fetal bovine serum (FBS) and grew till exponential phase. Bacterial suspension was aliquoted and stored in −80°C. The number of viable pneumococci was determined by the Miles and Misra Method. All culture media and supplements were from Oxoid, UK.

METHOD DETAILS

Mouse model of pneumococcal pneumonia

Mice were lightly anesthetized with O_2/isoflurane and inoculated (i.n.) with 1×10^6 colony-forming unit (CFU) of D39 in 50μL of sterile PBS as described previously.[54] For survival experiment, infected mice were monitored and scored regularly for signs of disease.[55] Mice that became lethargic were humanely culled with rising concentration of CO_2 and counted as death events. For the analysis of bacterial load and immune responses, blood, BAL and lung tissues were harvested at 18hrs post infection if not otherwise stated. Blood was taken by cardiac puncture or tail bleeding. BAL fluid was collected as previously described,[56] by inserting a catheter into the trachea and instilling 2 × 1mL of cold Hank's balanced salt solution (HBSS, Sigma Aldrich) with 100μM of EDTA (Fisher Scientific).

Treg cell depletion in DEREG mice

As described previously,[33] DEREG mice and wildtype littermates were intraperitoneally (i.p.) injected with 1μg of DT (Merck) in 100μL of sterile PBS for 2 consecutive days. The Treg cell depleting efficiency (>90%) was checked with lymphocytes isolated from lungs and cervical lymphoid nodes by the time of infection (24 h post second dose of DT) (Figure S1A).

IL-17A blockade in TNFR2$^{-/-}$ mice

Mice were treated (i.n.) with 50μg of anti-IL-17A monoclonal antibody (Clone 17F3, BioXCell) or isotype IgG1κ in 50μL of sterile PBS by the time of infection (antibody was mixed with the bacterial inoculum) and at 6 h post infection.

TNFR2$^+$ Treg cell sorting and adoptive transfer

Lymphocytes were isolated from spleens and lymph nodes of wildtype mice using described method.[57] Tissues were dissociated by pushing through a 70μm cell strainer and then subjected to red blood cell lysis to generate single cell suspension. CD4$^+$ T cells were separated by magnetic sorting through negative selection and then labeled with anti-mouse CD25-PE (7D4, Miltenyi Biotec) for positive selection of CD4$^+$CD25$^+$ T cells by Anti-PE Microbeads. Separated CD4$^+$CD25$^+$ T cells were labeled with anti-mouse CD127-BV421 (A7R34, BioLegend) and TNFR2-APC (REA228, Miltenyi Biotec) for the sorting of CD25$^+$CD127$^{-/low}$TNFR2$^+$ cells on BD FACSAria. CD4$^+$ T cell isolation kit and Anti-PE Microbeads both were from Miltenyi Biotec and the magnetic sorting was performed according to the manufacturer's instructions.

2×10^5 of sorted CD4$^+$CD25$^+$CD127$^{-/low}$TNFR2$^+$ cells were resuspended in 100μL of sterile PBS and intravenously (i.v.) injected into TNFR2$^{-/-}$ mouse. The control mice were i.v. injected with 100μL of sterile PBS. 24 h post cell transfer, all mice were i.n. infected with pneumococcus as described above.

Lung tissue processing

Lung tissues were harvested, cut into pieces, and digested in HBSS containing 300U/mL of type 1 collagenase (Gibco) and 75 μg/mL of DNase 1 (Sigma Aldrich), at 37°C for 1 h under constant horizontal shaking (200rpm). Digested lung pieces were then mechanically dissociated by pushing through a 70μm cell strainer and then subjected to red blood cell lysis to generate single cell suspension for restimulation and flow cytometry staining.

For bacterial quantification and cytokine measurement, the lung lobes were dissociated by an electronic tissue homogenizer (Ultra Turrax, IKA). The lung homogenates were centrifuged at 1500 xg for 10min to remove cells and tissue debris for the measurement of cytokine levels. TNFα concentration was determined using eBioscience Mouse TNF alpha ELISA Ready-SET-Go! Kit (Invitrogen) according to the manufacturer's instructions.

Quantification of pneumococcus

Viable counts of pneumococcus recovered from BAL, lung homogenates and blood were determined using the Miles and Misra method as described previously. Briefly, samples were serially diluted in sterile PBS and spotted on horse blood (5% v/v) supplemented BAB plates. Plates were incubated overnight at 37°C, 5% CO_2 and bacterial colonies were counted.

Flow cytometry

Single cells were incubated with Live/Dead Fixable Aqua Stain (Fisher Scientific) at 1:1000 to determine viable cells. Cell surface staining was performed with fluorochrome-conjugated anti-mouse monoclonal antibodies (mAbs) in the presence of True-Stain Monocyte Blocker (1:20) (BioLegend). For intranuclear transcription factor staining, cells were fixed and permeabilised with Foxp3/Transcription Factor Staining Buffer Set (Invitrogen) before incubation with corresponding mAbs. For intracellular cytokine detection, cells were stimulated with Cell Activation Cocktail, PMA/Ionomycin (with Brefeldin A) (BioLegend) for 4 h at 37°C, 5% CO_2 prior to staining. Following Live/Dead and cell surface staining, cells were fixed by IC Fixation Buffer (Invitrogen) and then washed with Permeabiliation Buffer (Invitrogen). Permeabilized cells were then stained with mAbs against intracellular cytokines. mAbs used in this study including CD45-PE-Cy7 (30-F11), CD3-FITC (17A2), CD11b-PE (M1/70), Ly6G-APC-Cy7 (1A8), NKp46-APC (29A1.4), SiglecF-BV421 (E50-2440), CD3-APC (17A2), CD4-APC-Cy7 (GK1.5), TCRγδ-PE-Cy7 (GL3), IL-17A-PE (TC11-18H10.1), IFNγ-BV421 (XMG1.2), CD3-PE-Cy7 (17A2), TNFR2-PE (TR75-89), CD44-APC (IM7), CD62L-Pacific Blue (MEL-14),

Foxp3-Alexa Fluor 488 (MF-14), all from BioLegend apart from SiglecF-BV421 which is from BD Biosciences. Stained samples were acquired on BD FACSCanto II and analyzed using Flowjo 10.4.

Lung T cell isolation and RT-qPCR

Lung cells isolated from 3 mice were pooled for the separation of T cells by magnetic sorting using CD90.2 Microbeads (Miltenyi Biotec). Purity of isolated T cells (>95%) was examine by flow cytometry staining with anti-mouse CD3-APC (17A2). Lung T cells were lysed with RLT buffer for mRNA extraction by RNeasy kit (Qiagen) according to the manufacturer's instructions. Total cDNA was synthesized from the purified mRNA using random primers and M-MLV reverse transcriptase (Promega). qPCR was performed using SYBR Green JumpStart Taq ReadyMix (Sigma Aldrich) on Bio-Rad CFX96 and normalised to *Hprt* using primers as below.

Il17a, 5′-CCAGCTGATCAGGACGCGCAAACATGAG-3′ (forward)
5′- TGAGGGATGATCGCTGCTGCCTTCACTG-3′ (reverse)
Hprt, 5′-GCAGTCCCAGCGTCGTGATTAGCGATGA-3′ (forward)
5′-CCCCTTGAGCACACAGAGGGCCACAATG-3′ (reverse)

Histology

Lungs were dissected and fixed with 10% neutral buffered formalin (Sigma Aldrich) and sent to LBIH Biobank, Liverpool for embedding, sectioning and hematoxylin and eosin (H&E) staining. Stained sample slides were scanned and examined using QuPath-0.2.3.

QUANTIFICATION AND STATISTICAL ANALYSIS

All data were analyzed and plotted using GraphPad Prism (version 9.0.1) software. Unpaired two-tailed *t* test or Mann-Whitney test was used to compare two datasets. Comparison of multiple datasets was carried out by ordinary two-way ANOVA with Sidak's multiple comparisons test. Survival curves was analyzed by Log rank (Mantel-Cox) test. Bacteria colony-forming unit (CFU) was log-transformed before analysis. Variance between datasets was tested in all analysis. Data are presented as mean ± SEM for bar graphs and dot plots unless otherwise stated, with sample size (n) specified in figure legends. Absolute p values are indicated in each figure. $p < 0.05$ is considered as statistically significant.